Kinetics of C_6H_5 Radical Reactions with Toluene and Xylenes by Cavity Ringdown Spectrometry

J. Park, D. Chakraborty, D. M. Bhusari, and M. C. Lin*

Department of Chemistry, Emory University, Atlanta, Georgia 30322

Received: January 5, 1999; In Final Form: March 23, 1999

The kinetics for the metathetical reactions of phenyl radical with toluene and xylenes have been studied experimentally and theoretically. The absolute bimolecular rate constants for the reactions of C_6H_5 with toluenes (C_7H_8 and C_7D_8) and xylenes (three C_8H_{10} isomers) were measured by cavity ringdown spectrometry at temperatures between 295 and 483 K. For the reaction with toluene, a strong isotope effect was observed, whereas for xylene reactions no structural preference was noticed among the three isomers. The weighted least-squares analysis of each reaction gave rise to the following rate constant expressions in units of cm^3/(mol s): $k(C_7H_8) = (2.08 \pm 0.11) \times 10^{11} \exp[-(1027 \pm 35)/T]$; $k(C_7D_8) = (2.27 \pm 0.43) \times 10^{11} \exp[-(1340 \pm 64)/T]$; $k(C_8H_{10}) = (1.48 \pm 0.11) \times 10^{11} \exp[-(526 \pm 27)/T]$. Additionally, we have carried out hybrid density functional theory (B3LYP) calculations for the reactions of C_7H_8 and C_7D_8 using the 6-31G-(d,p) basis set. The predicted rate constants using the conventional transition state theory with the calculated vibrational frequencies and moments of inertia fit well to the experimental results with only minor adjustments in the calculated reaction barriers. Combination of our low-temperature C_7H_8 kinetic data with those obtained at high temperatures in shock waves (ref 13) gave the expression $k(C_7H_8) = (4.15 \times 10^{-3})T^{4.5} \exp(800/T)$ cm^3/(mol s) for the temperature range 300−1450 K.

I. Introduction

The kinetics of aromatic radical reactions are relevant to the fundamental combustion chemistry of fossil fuels as well as to soot formation at its incipient stage. The small aromatic compounds such as toluene and xylenes are the key additives to unleaded gasoline, up to as much as 30 vol %.[1]

In our continuing effort to acquire basic kinetic data for phenyl radical reactions with hydrocarbon molecules[2−6] and with O_2,[7] made possible through our recent development of the ultrasensitive cavity ringdown spectroscopic (CRDS) technique[8,9] for kinetic applications, we have measured in the present study the absolute rate constants for its reactions with toluene (C_7H_8) and xylenes (C_8H_{10}, which include *o*-, *m*-, and *p*-isomers). To identify the dominant mechanism for the C_6H_5 attack on the toluene molecule, i.e., C−H abstraction from the methyl group vs ring addition, we have attempted to measure the rate constant for the reaction using nondeuterated and fully deuterated toluene in the present work to examine its kinetic isotope effect. We have also completed a kinetic measurement for the benzene (C_6H_6 and C_6D_6) reaction with C_6H_5 in our recent study.[10] Combination of these detailed kinetic data, aided by an additional quantum chemical calculation carried out for the $C_6H_5 + C_6H_6/C_6D_6$ ring addition process,[10] allows us to unambiguously elucidate the mechanisms of the titled reactions, as will be discussed in the following sections.

For the reaction of toluene with the phenyl radical, Stein and co-workers[11,12] have shown by a flow reactor study near 700 K that the major products of the reaction are benzene and benzyl radical occurring by the C−H abstraction mechanism. Recently, Heckmann et al.[13] have reported the rate constant, $k(C_7H_8) = 10^{13.9} \exp(-6014/T)$ cm^3/(mol s), with an unexpectedly high activation energy (12 kcal/mol) in the temperature range 1100−1450 K, employing the shock-tube/UV absorption spectrometric technique, monitoring the formation of benzyl radical at 260 nm. This result will be compared with our values obtained by the direct probing of C_6H_5 decay with CRDS later.

II. Experimental Section

Detailed descriptions of the CRDS technique for kinetic applications have been reported in our earlier publications.[2−7] To describe it briefly here, a heatable 50 cm long Pyrex flow tube, sealed at both the ends with highly reflective mirrors ($R = 0.9999$ and radius curvature of 6 m), formed the resonance cavity. A probing laser pulse with fwhm ≈ 10 ns introduced into the cavity perpendicular to both mirrors undergoes multiple (tens of thousands) internal reflections, effectively increasing its lifetime to 20−25 μs. The presence of absorbing species inside the cavity, however, reduces this photon decay time. The essence of the technique thus lies in measuring the variations in the photon decay time in the presence of varying concentrations of the reactant during the progress of the reaction of interest. In fact, the depletion in the reactant concentration with the progress of reaction is determined by measuring the increase in photon decay time during the reaction.

For the present study of the reactions of the C_6H_5 radical, two lasers were used for the generation of the radical and its detection. A 248 nm KrF excimer laser (Lambda Physik LPX105) was used for the generation of the phenyl from the photodissociation of nitrosobenzene, with the two-splitted laser beams crossing at the center of the reactor at a 30° angle. An excimer laser (Lambda Physik EMG 102) pumped tunable dye laser (Lambda Physik FL 3002) was used to measure the decay of phenyl radical at 508.0 nm. A small fraction of the probing photon pulse transmitted through the second mirror was directly detected by a Hamamatsu photomultiplier tube (PMT). The PMT signal was acquired and averaged by using a lock-in multichannel digital oscilloscope (LeCroy 9310M). A pulse-delay generator (SRC DG 535) interfaced with a computer was used to control the delay time between the photodissociation and

* Corresponding author. E-mail address: chemmcl@emory.edu.

10.1021/jp990049v CCC: $18.00
Published on Web 04/22/1999

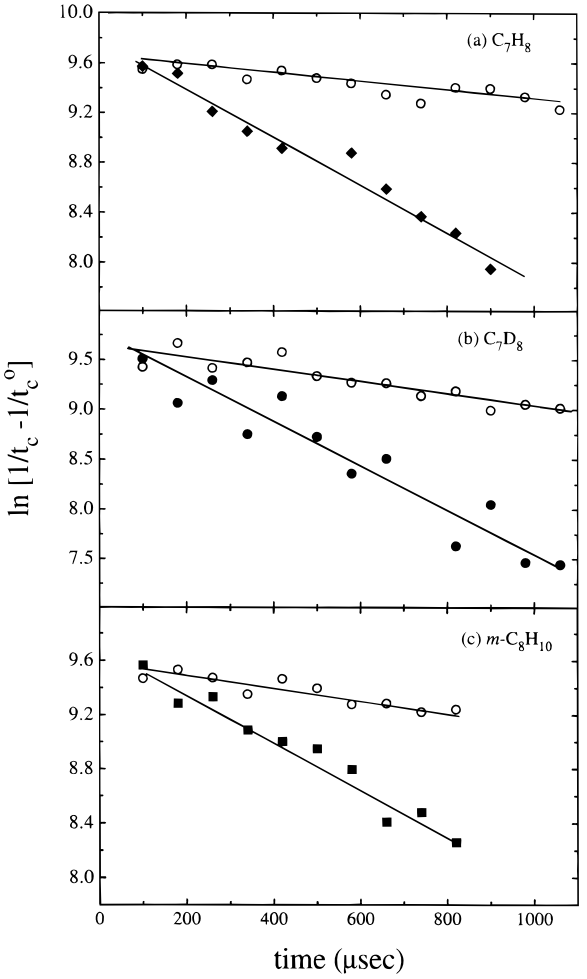

Figure 1. Typical pseudo-first-order decay plots of C_6H_5 measured under various conditions at 297 K: (○) [X] = 0; (◆) [C_7H_8] = 1.37 × 10^{-7} mol/cm^3; (●) [C_7D_8] = 3.78 × 10^{-7} mol/cm^3; (■) [C_8H_{10}] = 6.11 × 10^{-8} mol/cm^3.

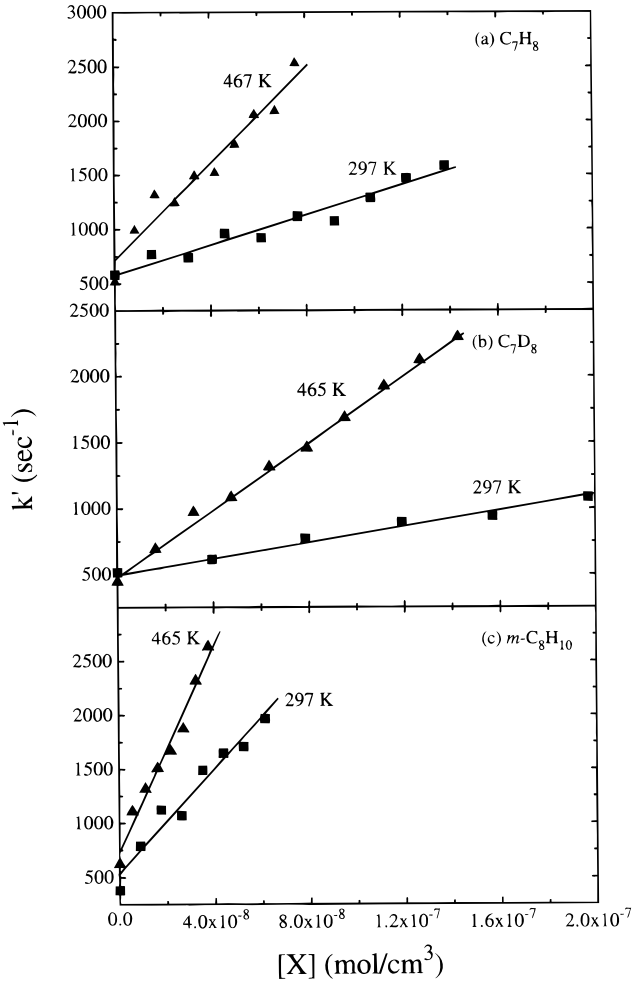

Figure 2. k' vs [X] for the C_6H_5 + C_7H_8, C_7D_8, and C_8H_{10} reactions measured at the specified temperatures.

probe lasers and to trigger the data acquisition system. Typically, 40 pulses were collected at a rate of 2 Hz for each time delay.

On the basis of the aforementioned principle, it can be shown that if the chemical decay time (t') of the radical is long enough compared to the photon decay time, then the following relationship holds:[2−7]

$$\ln(1/t_c - 1/t_c^o) = B - k't' \quad (1)$$

where t_c^o is the photon decay time measured in the absence of C_6H_5 and t_c is the photon decay time after a finite time interval after the photodissociation of C_6H_5NO. B is the experimental constant that depends on the cavity length, the extinction coefficient, refractive index of the reaction medium, and initial concentration of C_6H_5. Under the present experimental conditions, t' was of the order of 800−1000 μs while t_c^o was of the order of 20−30 μs. When the quantity $\ln(1/t_c - 1/t_c^o)$ is plotted against the delay time for a constant concentration of X, the slope of the straight line gives the pseudo-first-order rate constant k', as shown in Figure 1. The magnitude of k' varies with the concentration of the reactant X according to the equation

$$k' = k^o + k''[X] \quad (2)$$

where k^o is the decay constant of the radical measured in the absence of X and k'' is the bimolecular rate constant for C_6H_5 + X. Thus, k'' can be obtained directly from the slope of k' vs [X] as shown in Figure 2.

The radical source, nitrosobenzene (Aldrich 97%), was recrystallized using ethanol as solvent and vacuum-dried before use. The reactants (C_7H_8, C_7D_8, and C_8H_{10} isomers; Aldrich, 99.5%) were purified by trap-to-trap distillation. The Ar (Specialty Gases, 99.999%) carrier gas was used without further purification.

III. Results and Discussion

The bimolecular rate constants determined from the slopes of k' vs concentration plots as illustrated in Figure 2 are summarized in Table 1 for C_6H_5 reactions with C_7H_8 and C_7D_8 and *o*-, *m*-, and *p*-C_8H_{10}. These data are also graphically presented in Figure 3 for comparison with existing rate constants for benzene,[10] toluene,[11,13−15] and xylene[11,14,15] reactions. For the xylene reactions no isomeric specificity is noted, as illustrated in the Arrhenius plot presented in the figure. Weighted least-squares analysis of the individual set of reaction rate constants gave rise to the following expressions, in units of cm^3/(mol s),

$$k(C_7H_8) = (2.08 \pm 0.11) \times 10^{11} \exp[-(1027 \pm 35)/T] \quad (3)$$

$$k(C_7D_8) = (2.27 \pm 0.43) \times 10^{11} \exp[-(1340 \pm 64)/T] \quad (4)$$

$$k(C_8H_{10}) = (1.48 \pm 0.11) \times 10^{11} \exp[-(526 \pm 27)/T] \quad (5)$$

for the temperature range 295−483 K. The uncertainties given

TABLE 1: Measured Bimolecular Rate Constants of C_6H_5 Reactions with Toluene (C_7H_8), Toluene-d_8 (C_7D_8), and Xylenes (*o*-, *m*-, *p*-C_8H_{10})

reactant, X	*T* K	*P* Torr	[RH] × 10^8 mol/cm^3	$k/10^{10}$ cm^3/(mol s)[a]
C_7H_8	295	30.0	0−10.9	0.69 ± 0.19
	297	17.6	0−13.7	0.62 ± 0.19
	297	17.6	0−13.7	0.68 ± 0.22
	321	30.0	0−8.66	0.84 ± 0.22
	340	17.6	0−10.9	0.96 ± 0.22
	343	30.0	0−10.9	1.08 ± 0.19
	349	17.6	0−10.5	1.08 ± 0.29
	368	17.6	0−10.1	1.20 ± 0.32
	372	30.0	0−10.5	1.24 ± 0.22
	397	17.6	0−9.30	1.55 ± 0.15
	419	30.0	0−10.9	1.79 ± 0.22
	426	17.6	0−8.70	1.79 ± 0.15
	467	17.6	0−6.76	2.25 ± 0.38
	473	30.0	0−9.27	2.65 ± 0.22
C_7D_8	297	30.0	0−37.8	0.28 ± 0.03
	309	30.0	0−19.7	0.29 ± 0.09
	341	17.4	0−19.4	0.40 ± 0.09
	367	17.4	0−15.3	0.60 ± 0.06
	377	30.0	0−13.3	0.60 ± 0.21
	414	17.4	0−16.8	0.82 ± 0.21
	428	30.0	0−13.3	0.99 ± 0.21
	436	17.4	0−15.5	1.18 ± 0.13
	453	30.0	0−25.6	1.23 ± 0.09
	465	17.4	0−14.5	1.27 ± 0.09
m-C_8H_{10}	295	30.0	0−7.80	2.42 ± 0.39
m-C_8H_{10}	297	5.7	0−6.11	2.73 ± 0.39
p-C_8H_{10}	318	30.0	0−0.89	2.71 ± 0.59
p-C_8H_{10}	329	5.7	0−4.85	3.00 ± 0.59
o-C_8H_{10}	357	5.7	0−4.29	3.38 ± 0.48
m-C_8H_{10}	374	5.7	0−4.27	3.54 ± 0.40
o-C_8H_{10}	397	5.7	0−4.14	3.81 ± 0.38
m-C_8H_{10}	403	30.0	0−3.79	4.05 ± 0.39
p-C_8H_{10}	411	5.7	0−6.00	3.87 ± 0.59
p-C_8H_{10}	432	5.7	0−3.71	4.53 ± 0.79
m-C_8H_{10}	462	5.7	0−3.54	4.88 ± 0.51
p-C_8H_{10}	483	30.0	0−0.59	5.04 ± 0.51

[a] The uncertainties represent 1σ, evaluated with weighted least-squares analyses by convoluting the errors in k' for k''.

above were evaluated by convoluting the errors in both k' and k'' through the weighted least-squares analysis.

1. C_6H_5 + Toluene. The reaction of C_6H_5 with toluene was found to have a strong isotope effect with $k_H/k_D = 2.6$ at 300 K and 1.7 at 500 K. As the rate constant for the addition of C_6H_5 to the benzene ring is about a factor of 2 slower at 500 K and a factor of 6 slower at 300 K, according to the results of our recent experimental and theoretical study[10] (see Figure 3), the observed kinetic isotope effect in the toluene reaction suggests that the reaction occurs primarily by C−H(D) abstraction from the methyl group. Stein and co-workers[12] have previously determined the relative rates of H-abstraction vs phenylation for $C_6H_5 + C_7H_8$ at different ring sites at 723 K by GC/MS product analysis. They found that the abstraction rate is a factor of 10−20 greater, depending on the phenylation sites. This result is qualitatively consistent with the present data mentioned above.

For the $C_6H_5 + C_6H_6/C_6D_6$ reactions studied by CRDS,[10] we did not detect any measurable kinetic isotope effect and the activation energy for the ring addition process was determined to be 3.8 kcal/mol, which is almost twice higher than that for the reaction with C_7H_8.

For the toluene reaction, Heckmann et al.[13] have recently reported the rate constant

$$k(C_7H_8) = 7.94 \times 10^{13} \exp(-6014/T)\ \text{cm}^3/(\text{mol s})$$

obtained by shock-tube/UV absorption spectrometry in the 1100−1450 K temperature range, as alluded to before, with a significantly larger activation energy (12 kcal/mol) compared with our value of 2.0 kcal/mol. Their result is also plotted in Figure 3 for comparison with our data, with and without isotope labeling. At first sight the large deviation between the two sets of kinetic data is puzzling and requires a detailed theoretical investigation (vide infra).

For C−H abstraction reactions by C_6H_5, we had earlier investigated its reactions with cycloalkanes (*c*-C_5H_{10} and *c*-C_6H_{12})[5] and small alkanes containing tertiary CH bonds (isobutane, diisopropyl, and 2,3,4-trimethylpentane)[6] by CRDS in the same temperature range. For C_6H_5 + cycloalkanes, we have reported the activation energies to be 4.1 kcal/mol for *c*-C_5H_{10} and 3.8 kcal/mol for *c*-C_6H_{12}, while for the reactions with isobutane, diisopropyl, and 2,3,4-trimethylpentane containing one, two, and three *t*-CH bonds, respectively, we have determined their activation energies to be 3.0, 2.0, and 0.85 kcal/mol. These values are closer to that found in the toluene reaction. The *t*-CH bond strength in *i*-C_4H_{10} is stronger than that of the first methyl CH bond in toluene by about 8 kcal/mol. Accordingly, one would expect a slightly higher activation energy for the *i*-C_4H_{10} reaction, as was found in our study.

2. C_6H_5 + Xylenes. The absolute rate constants for the xylene reactions with the phenyl radical in the gas phase were measured for the first time in this work. The three isomers of xylene have essentially the same reactivity toward C_6H_5, with a somewhat smaller activation energy (1.0 kcal/mol) compared with that of the toluene reaction (2.0 kcal/mol). At room temperature, the absolute rate constant for the xylene reactions is about three and half times higher than that for the toluene reaction because of the greater number of the CH bonds and the lower activation energy. The difference, however, narrows noticeably at higher temperatures (see Figure 3) with $k(C_8H_{10})/k(C_7H_8) = 2.0$ at 500 K, for example. A similar trend was also observed in the C_6H_5 reactions with the *t*-CH containing alkanes, from isobutane to 2,3,4-trimethylpentane.[6] This interesting phenomenon deserves a close examination at the molecular level by means of quantum chemical calculations employing a moderately high-level ab initio method, which, unfortunately, still requires a considerable amount of supercomputer CPU time at present.

The fact that the C_6H_5 radical exhibits the same reactivity toward the three xylene isomers is perhaps not surprising, in view of the absence of steric hindrance and the high reactivity of the phenyl. Even for CH_3, which is less reactive than C_6H_5, the relative rate constants for its reactions with the xylene isomers to that for $CH_3 + H_2$ at temperatures 955−980 K were found to be essentially the same (5.3 ± 0.1).[16]

For the C_6H_5 reaction with *p*-C_8H_{10}, Fahr and Stein[11] have measured its rate constants for the H-abstraction and the phenylation processes (displacing H and CH_3) relative to that for the H-displacement at 723 K. A similar determination was made for those of H-abstraction and H-displacement by C_6H_5 at the ortho, meta, and para positions in toluene relative to that of the H-displacement in the *p*-xylene reaction. Combination of the ratio of the sum of these product branching rate constants for the *p*-xylene and toluene reactions, $k(C_8H_{10})/k(C_7H_8) = 1.72$ at 723 K, with our absolute rate constant for the toluene reaction calculated at the same temperature gives $k(C_8H_{10}) = 8.30 \times 10^{10}$ cm^3/(mol s). This value, given in Figure 3 with a solid diamond, agrees closely with our xylene CRDS data extrapolated to 723 K.

3. Comparison with Solution Kinetic Data. The rates of the reactions of C_6H_5 with C_7H_8 and *p*-C_8H_{10} have been determined in solution at 333 K by Bridger and Russell relative

TABLE 2: Total Energies (ZPE-Corrected), Moments of Inertia, and Vibrational Frequencies of the Reactants, Transition States, and Products Calculated at B3LYP/6-31G(d,p) Level of Theory

species	energy (AU)	I_i (AU)	ν_i (cm^{-1})
$C_6H_5CH_3$	−271.450 77	326.0, 719.1, 1033.9	33, 211, 343, 417, 477, 528, 636, 712, 747, 801, 860, 912, 970, 995, 1005, 1017, 1057, 1066, 1118, 1186, 1209, 1235, 1346, 1362, 1426, 1482, 1502, 1516, 1542, 1642, 1362, 1426, 1482, 1502, 1516, 1542, 1642, 1665, 3036, 3096, 3124, 3168, 3170, 3182, 3191, 3204
C_6H_5	−231.481 74	287.8, 322.2, 609.9	402, 428, 600, 618, 673, 724, 817, 892, 961, 985, 990, 1023, 1057, 1080, 1181, 1181, 1313, 1342, 1472, 1484, 1592, 1645, 3172, 3178, 3191, 3194, 3204
TS	−502.930 29	991.5, 5326.7, 5674.8	1076i,[a] 6, 27, 28, 82, 108, 204, 334, 402, 406, 409, 418, 500, 514, 537, 612, 635, 687, 709, 718, 730, 764, 815, 838, 857, 901, 916, 960, 971, 993, 995, 1011, 1015, 1015, 1039, 1055, 1078, 1086, 1100, 1121, 1183, 1186, 1189, 1208, 1249, 1322, 1341, 1342, 1363, 1377, 1425, 1483, 1483, 1494, 1504, 1538, 1609, 1631, 1641, 1656, 3083, 3154, 3167, 3171, 3172, 3174, 3182, 3185, 3187, 3192, 3200, 3205
$C_6H_5CH_2$	−270.811 40	326.2, 668.9, 995.1	203, 357, 391, 481, 505, 538, 627, 684, 707, 774, 833, 835, 898, 965, 977, 987, 995, 1042, 1123, 1180, 1192, 1296, 1343, 1360, 1485, 1505, 1517, 1592, 1614, 3165, 3174, 3176, 3188, 3193, 3207, 3264
C_6H_6	−232.157 64	317.3, 317.3, 643.7	415, 415, 625, 621, 694, 710, 865, 865, 970, 974, 1013, 1016, 1019, 1066, 1065, 1180, 1202, 1209, 1354, 1381, 1523, 1524, 1652, 1652, 3170, 3180, 3188, 3196, 3196, 3206

[a] Stands for imaginary frequency.

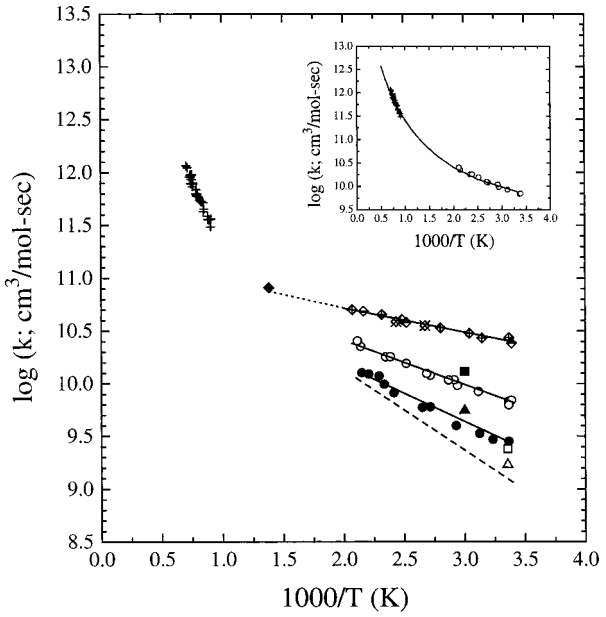

Figure 3. Arrhenius plots for $C_6H_5 + C_7H_8$ (○), C_7D_8 (●), and C_8H_{10} (◇) (− center, *m*-C_8H_{10}; × center, *p*-C_8H_{10}; + center, *o*-C_8H_{10}). Solid line, least-squares fittings; dashed line, ref 10 for $C_6H_5 + C_6H_6$; dotted line, extension of these studies for the $C_6H_5 + C_7H_8$ reaction; +, ref 13 for the $C_6H_5 + C_7H_8$ reaction; ◆, ref 11 for the $C_6H_5 + C_8H_{10}$ reaction; ■ and □, refs 14 and 15 for the $C_6H_5 + C_8H_{10}$ reaction; ▲ and △, refs 14 and 15 for the $C_6H_5 + C_7H_8$ reaction. Inset: Least-squares analysis of our low-temperature C_7H_8 kinetic data with those of Heckmann et al. (ref 13). The smooth curve can be given by $k(C_7H_8) = (4.15 \times 10^{-3})T^{4.5} \exp(800/T)$ $cm^3/(mol\ s)$.

to that of the $C_6H_5 + CCl_4 \rightarrow C_6H_5Cl + CCl_3$ reaction.[14] Using our absolute rate constant for the CCl_4 reaction,[5] we have converted their relative rates to give $k(C_7H_8) = 5.54 \times 10^9$ and $k(C_8H_{10}) = 1.30 \times 10^{10}$ $cm^3/(mol\ s)$ at 333 K. These values, as shown in Figure 3, are about a factor of 2 lower than our gas-phase results calculated by eqs 3 and 5. In a different experiment carried out in Freon 113 at 298 K by Scaiano and Stewart,[15] using an optically active aromatic radical generated by a concurrent C_6H_5 reaction as a monitor, the two rate constants were reported to be $(1.7 \pm 0.7) \times 10^9$ and $(2.4 \pm 0.1) \times 10^9$ $cm^3/(mol\ s)$ at room temperature. These values, also shown in Figure 3, are smaller than our corresponding results by a factor of 4 and 10 according to eqs 3 and 5.

The deviations noted above between the gas-phase and solution data are puzzling. Earlier, we had compared our gas-phase results with those obtained in solution by the same authors cited above for the C_6H_5 reactions with O_2, *c*-C_5H_{10}, *c*-C_6H_{12}, and CCl_4;[5] we noted the existence of self-consistency and reasonable agreement between the gas-phase and solution data using our absolute rate constants for these reactions to check the relative rate constants measured in solution.[5] It is worth noting that in the list of compounds given above none of them is aromatic.

4. Theoretical Calculation for the CH Abstraction Reaction. To reconcile the apparent large discrepancy between our low-temperature toluene result and that measured at high temperatures by Heckmann et al.[13] and the large deviations noted above between the gas-phase and solution data, we have carried out a theoretical calculation for the rate constants of the abstraction reaction involving both C_7H_8 and C_7D_8. On account of the large size of the system, we employed the hybrid density functional theory (B3LYP) using Becke's three-grid integration and exchange functional[17] with the nonlocal correlation functional of Lee, Yang, and Parr[18] using the 6-31G(d,p) Gaussian basis set.[19] The energies, vibrational frequencies, and moments of inertia calculated with the B3LYP/6-31G(d,p) method, summarized in Table 2, were employed for prediction of the rate constants using the conventional transition state theory (TST).[20]

Figure 4 presents the geometries of the reactants, products, and the TS, and Figure 5 shows the schematic energy curves for the C_7H_8 and C_7D_8 systems relative to the $C_6H_5 + C_7H_8$ reactant energy. The calculated transition barrier for the $C_6H_5 + C_7H_8$ reaction is 1.4 kcal/mol at the B3LYP level of theory as shown in Figure 5, whereas the deuterated analogue has an activation barrier of 2.2 kcal/mol. On account of the presence of four low-vibrational frequencies (see Table 2) associated with the torsional vibrations of the two phenyl rings (6 and 82 cm^{-1}) and the rocking motions of the phenyl and benzyl groups (27 and 28 cm^{-1}), as illustrated by the pictures of atomic motions in Figure 6, we have substituted these low-frequency modes with one free and one restricted internal rotor and one 2-D hindered rotor, respectively, in our partition function calculations, using the methods described by Troe[21] and Hase and

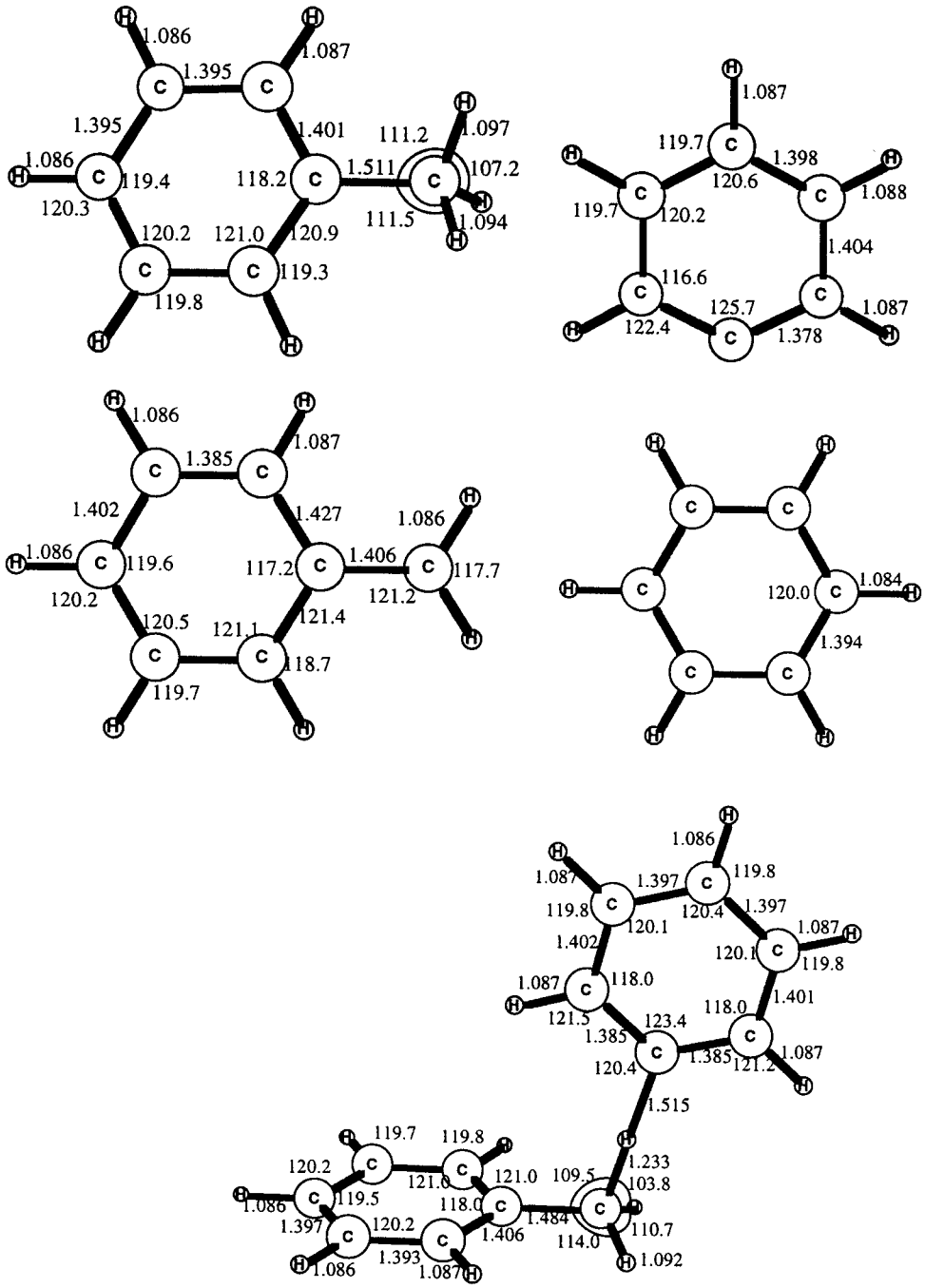

Figure 4. Molecular and transition state geometries, optimized at the B3LYP/6-31G(d,p) level of theory. Bond lengths are in angstroms and angles in degrees.

Zhu.[22] For the torsional motions, the 6 cm^{-1} vibration of the attacking C_6H_5, which has an estimated barrier of 0.1 kcal/mol, is essentially a free rotor with a calculated reduced moment of inertia of 108.74×10^{-40} g cm^2. The 82 cm^{-1} torsional vibration of the benzyl, however, has an estimated barrier of 19 kcal/mol; it can be correctly treated either as a harmonic oscillator or as a restricted rotor. For the two low-frequency rocking vibrations, our estimated reduced moment of inertia, 153.46×10^{-40} g cm^2, gave rise to an effective barrier of 5.93 kcal/mol. However, the 2-D hindered rotor partition function calculated using the equation of Hase and Zhu[22] gave essentially the same values as those predicted by the vibrational partition functions. Figure 7 compares the measured and calculated (B3LYP/6-31G-(d,p)-TST) results for both C_7H_8 and C_7D_8. To fit the predicted rate constants to experimental results, we adjusted the calculated energy barrier of the transition states from 1.4 to 0.9 kcal/mol for C_7H_8 and from 2.2 to 1.6 kcal/mol for C_7D_8. These adjustments are well within the uncertainty of the B3LYP method for energy prediction.[23] The calculated values with the Eckart type tunneling corrections[24] give the expressions in the temperature range 300−2000 K of $k(C_7H_8) = 0.26T^{4.02} \exp[290/T]$ and $k(C_7D_8) = 0.58T^{3.95} \exp[-144/T]$ cm^3/(mol s). For C_7H_8 the predicted rapid increase in the rate constant above 1000 K reasonably accounts for the large activation energy reported by Heckmann et al.[13] in their shock-tube study. In view of this theoretical justification, we combined our low-temperature C_7H_8 data with the high-temperature shock-tube results in our final least-squares analysis (see the inset in Figure 3), which yields $k(C_7H_8) = (4.15 \times 10^{-3})T^{4.5} \exp(800/T)$ cm^3/(mol s). This expression is recommended for kinetic modeling of soot formation in hydrocarbon combustion.

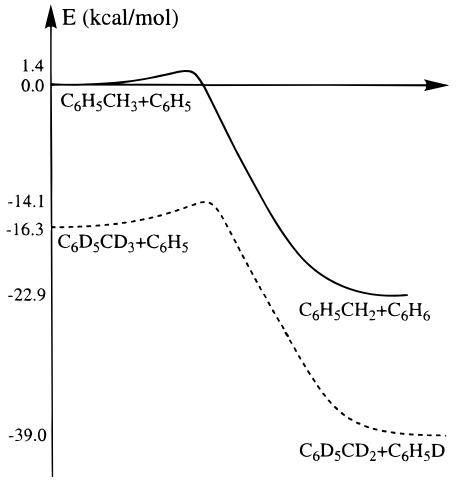

Figure 5. Potential energy profiles calculated at the B3LYP/6-31G-(d,p) level for the $C_6H_5 + C_7H_8$ and C_7D_8 reactions.

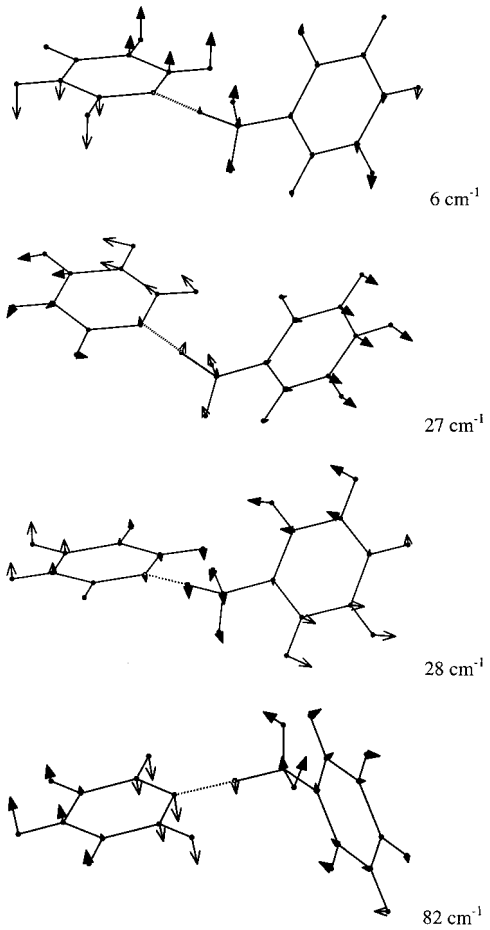

Figure 6. Some critical vibrational modes of the transition state.

IV. Concluding Remarks

The absolute rate constants for the reactions of C_6H_5 with toluene (C_7H_8 and C_7D_8) and the three xylene structural isomers have been measured by cavity ringdown spectrometry in the temperature range 295−483 K. The observation of a strong primary kinetic isotopic effect in the C_7H_8 and C_7D_8 reactions reveals that the C_6H_5 + toluene reaction in this temperature range takes place primarily by direct C−H abstraction from the CH_3 group, confirming the result of Stein and co-workers studied by GC/MS[12] and the result of Heckmann et al.[13] by the UV detection of the benzyl radical. The large difference in the activation energies determined for C_7H_8 and C_7D_8 (2.0 and 2.6 kcal/mol, respectively) from that obtained by Heckmann et al.[13] in a shock-tube study at $1100 \leq T \leq 1450$ K (12 kcal/mol) could be accounted for by the rapid increase in the rate constant with temperature, as predicted by our quantum chemical and TST calculations. Combination of the two sets of toluene kinetic data yields $k(C_7H_8) = (4.15 \times 10^{-3})T^{4.5} \exp(800/T)$ cm^3/(mol s) for the temperature range 300 K $\leq T \leq$ 1450 K.

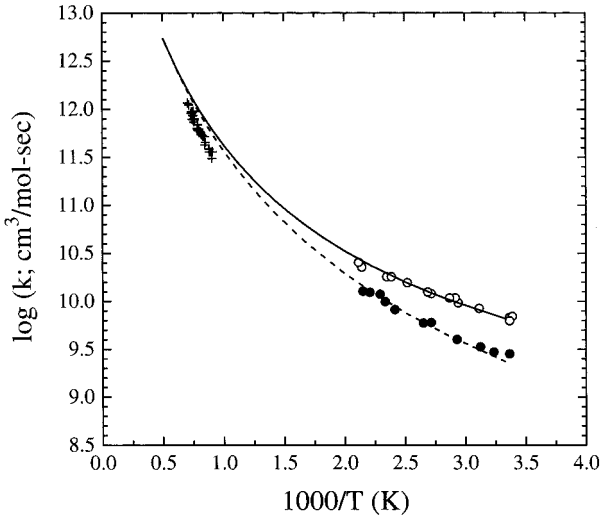

Figure 7. Comparison of the experimentally measured and theoretically predicted results by B3LYP/6-31G(d,p)-TST calculations for the $C_6H_5 + C_7H_8$ (○ and solid curve) and C_7D_8 reactions (● and dashed curve). +, ref 13 for the $C_6H_5 + C_7H_8$ reaction. For the TST calculations, $E_0 = 0.9$ kcal/mol for C_7H_8 and $E_0 = 1.6$ kcal/mol for C_7D_8 were used.

The results of our study of the xylene isomeric reactions with C_6H_5 reveal no structural dependence. The extrapolation of our low-temperature toluene and xylene data to 723 K led to a good agreement with the relative rate constant of Stein and co-workers, $k_{C8H10}/k_{C7H8} = 1.72$ measured at the same temperature.[12]

For both toluene and xylene reactions with C_6H_5, limited solution kinetic data have been measured by means of a conventional relative rate method[14] or a photometric method using a competitive reaction that generates an optically active species.[15] These condensed phase data disagree with the present gas-phase results noticeably, contrary to the good agreement reported previously for the C_6H_5 reactions with *c*-C_5H_{10}, *c*-C_6H_{12}, CCl_4, and O_2.[5,7]

Acknowledgment. The authors are grateful for the support of this work from the Basic Energy Sciences, Department of Energy, under Contract No. DE-FG02-97-ER14784. We are also thankful to Dr. W. H. Kirchhoff for providing us sufficient NERSC CPU time for the lengthy ab initio MO calculations.

References and Notes

(1) Sawyer, R. F. *Symp. (Int.) Combust.*, [*Proc.*], *24th* **1992**, 1423.
(2) Yu, T.; Lin, M. C. *J. Am. Chem. Soc.* **1993**, *115*, 4371.
(3) Yu, T.; Lin, M. C. *Int. J. Chem. Kinet.* **1994**, *26*, 1095.
(4) Yu, T.; Lin, M. C. *Combust. Flame* **1995**, *100*, 169.
(5) Yu, T.; Lin, M. C. *J. Phys. Chem.* **1995**, *99*, 8599.
(6) Park, J.; Gheyas, S. I.; Lin, M. C.; *Int. J. Chem. Kinet.*, submitted.
(7) Yu, T.; Lin, M. C. *J. Am. Chem. Soc.* **1994**, *116*, 9571.
(8) O'Keefe, A.; Deacon, D. A. G. *Rev. Sci. Instrum.* **1988**, *59*, 2544.

(9) O'Keefe, A.; Scherer, J. J.; Cooksy, A. L.; Sheeks, R.; Heath, J.; Saykally, R. J. *Chem. Phys. Lett.* **1990**, *172*, 214.

(10) Park, J.; Burova, S.; Rodgers, A.; Lin, M. C. Experimental and Theoretical Studies for the $C_6H_5 + C_6H_6$ Reaction: Effects of Temperature and Pressure on the Forward and Reverse Processes. In preparation.

(11) Fahr, A.; Stein, S. E. *J. Phys. Chem.* **1988**, *92*, 4951.

(12) Chen, R. H.; Kafafi, S. A.; Stein, S. E. *J. Am. Chem. Soc.* **1989**, *111*, 1418.

(13) Heckmann, E.; Hippler, H.; Troe, J. *Symp. (Int.) Combust., [Proc.], 26th* **1996**, 543.

(14) Bridger, R. F.; Russel, G. L. *J. Am. Chem. Soc.* **1963**, *85*, 3754.

(15) Scaiano, J. C.; Stewart, L. C. *J. Am. Chem. Soc.* **1983**, *105*, 3609.

(16) Burr, J. G.; Strong, J. D. *J. Am. Chem. Soc.* **1964**, *86*, 5065.

(17) Becke, A. D. *J. Chem. Phys.* **1993**, *98*, 5648. (b) Becke, A. D. *J. Chem. Phys.* **1992**, *96*, 2155. (*c*) Becke, A. D. *J. Chem. Phys.* **1992**, *97*, 9173.

(18) Lee, C.; Yang, W.; Parr, R. G. *Phys. Rev. B* **1988**, *37*, 785.

(19) Frisch, M. J.; Trucks, G. W.; Schlegel, H. B.; Gill, P. M. W.; Johnson, B. G.; Robb, M. A.; Cheeseman, J. R.; Keith, T.; Petersson, G. A.; Montgomery, J. A.; Raghavachari, K.; Al-Laham, M. A.; Zakrzewski, V. G.; Ortiz, J. V.; Foresman, J. B.; Cioslowski, J.; Stefanov, B. B.; Nanayakkara, A.; Challacombe, M.; Peng, C. Y.; Ayala, P. Y.; Chen, W.; Wong, M. W.; Andres, J. L.; Replogle, E. S.; Gomperts, R.; Martin, R. L.; Fox, D. J.; Binkley, J. S.; Defrees, D. J.; Baker, J.; Stewart, J. P.; Head-Gordon, M.; Gonzalez, C.; Pople, J. A. *GAUSSIAN 94*, revision D.3; Gaussian, Inc.: Pittsburgh, PA, 1995.

(20) Laidler, K. J. *Chemical Kinetics*, 3rd ed.; Harper and Row: New York, 1987.

(21) Troe, J. *J. Chem. Phys.* **1977**, *66*, 4758.

(22) Hase, W. J.; Zhu, L. *Int. J. Chem. Kinet.* **1994**, *26*, 407.

(23) Mebel, A. M.; Morokuma, K.; Lin, M. C. *J. Chem. Phys.* **1995**, *103*, 7414.

(24) Eckart, C. *Phys. Rev.* **1930**, *35*, 1303.